THE RECORDING OF INTERANNUAL CLIMATIC CHANGE BY HIGH-RESOLUTION NATURAL SYSTEMS: TREE-RINGS, CORAL BANDS, GLACIAL ICE LAYERS, AND MARINE VARVES

Tim R. Baumgartner[1]
Joel Michaelsen[2]
Lonnie G. Thompson[3]
Glen T. Shen[4]
Andy Soutar[5]
Richard E. Casey[6]

Abstract. Large-scale climatic variability associated with the El Niño-Southern Oscillation phenomenon is recorded by tree-rings of the semiarid United States and Mexico, coral bands from the Galapagos Islands, glacial ice layers from a Peruvian ice cap, and varved sediments in the Santa Barbara Basin and the Gulf of California. Because of their differences in location, environmental setting, and recording mechanisms, integration of the study of these natural high-resolution systems provides a rich potential for documenting the multiple aspects of the El Niño-Southern Oscillation history prior to instrumental recording. As a first step towards this integrated approach we have assembled a critical selection of modern high-resolution proxy records available from these systems for the 50-year period beginning in 1935. The principal goal of this paper is to describe the mechanisms, their relative sensitivities, and the recording response of each proxy system to large-scale interannual climatic variability represented by an instrumental record of the Southern Oscillation. Results show that systems with high climatic sensitivity have one or more recording mechanism exhibiting low persistence and rapid response to interannual variability, and whose response is restricted to a single, local environmental process, which is itself strongly coupled to large-scale climatic forcing.

Introduction

A variety of phenomena generate permanent records of natural processes that are governed by climate. Information obtained from such indirect preservation of climatic history is generally referred to as proxy data to distinguish it from direct instrumental measurement. The natural recording phenomena, or systems, that are commonly used to reconstruct proxy climatic histories can be grouped into two major categories (Figure 1) based on whether they provide episodic or continuous records of climatic variability [U.S. Committee for Global Atmospheric Research Program, 1975]. Depending upon the temporal scale of variability preserved, the continuous records can be further classified as low-, intermediate-, and high-resolution.

Continuous low-resolution systems are best exemplified by depositional environments in the deep sea with relatively slow sedimentation rates (2–5 cm per 1000 years) and by the deep sections of the polar ice sheets. (While the polar ice yields records spanning up to a million years, thinning by glacial flow continually reduces their temporal resolution.) These systems preserve the traces of climatic change occurring over millennial time scales and are well suited to investigation of the glacial-interglacial variability within the Quaternary. Resolution of centennial through decadal variability (the intermediate scale), is preserved in the intermediate depths of polar ice (older than 10,000 years) and from lake and marine sediments along continental margins where sedimentation rates reach values of 10–100 cm per 1000 years.

Continuously recording, high-resolution systems all generate visibly distinct layering as a response to climatic variation from one season to the next. High-resolution records result from the growth of living organisms which produce structures such as tree-rings and coral banding, or from complex depositional processes producing dust layers within glacial ice, and the lamina couplets in varved marine or fresh water sediments. The dominant climatic signal preserved in these records is, therefore, that of the annual cycle. These systems are, however, particularly valuable for their preservation of the year-to-year, or interannual, scale of climatic variability as the deviation in system response from the annual cycle. Although they possess a lower fidelity in their recording response to climatic variation, high-resolution proxy records can be considered natural extensions of the instrumental record. These natural systems may also store environmental information by more than one mechanism, thus providing several proxy variables as separate recording channels.

The purpose of this paper is to examine the relative sensitivities to large-scale interannual climatic change over a range of high-resolution natural systems. To accomplish this we compare the proxy records of five high-resolution systems from the eastern Pacific Ocean and the western regions of North and South America (Figure 2). These include a tropical ice cap in Peru, equatorial corals from the Galapagos Islands, semiarid forests in North America, and marine varved sediments from two coastal seas off North America. Since all these systems are situated within oceanographic or atmospheric regimes that are influenced by the El Niño-Southern Oscillation (ENSO) phenomenon [Cane, 1983; Rasmussen and Wallace,

[1]Centro de Investigación Científica y de Educación, Superior de Ensenada, Ensenada, Baja California, MEXICO.
[2]Department of Geography, University of California, Santa Barbara, Santa Barbara, CA, U.S.A.
[3]Institute for Polar Studies, Ohio State University, Columbus, OH, U.S.A.
[4]Lamont-Doherty Geological Observatory, Columbia University, Palisades, NY, U.S.A.
[5]Scripps Institution of Oceanography, University of California, San Diego, La Jolla, CA, U.S.A.
[6]Marine Studies Program, University of San Diego, San Diego, CA, U.S.A.

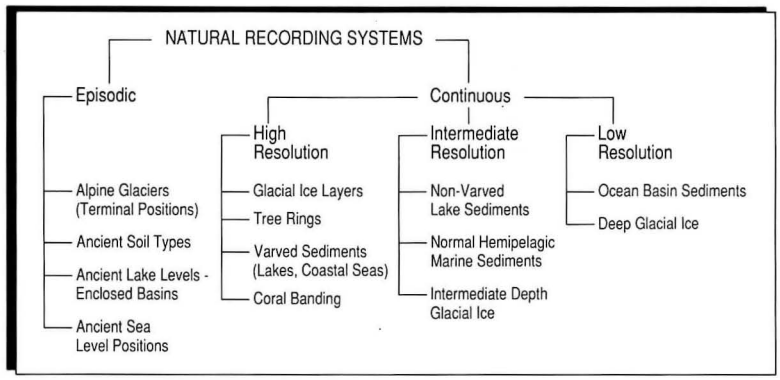

Fig. 1. Classification of proxy climatic recording phenomena into episodic and continuous natural recording systems. Continuous recording systems are subdivided based on their temporal resolution.

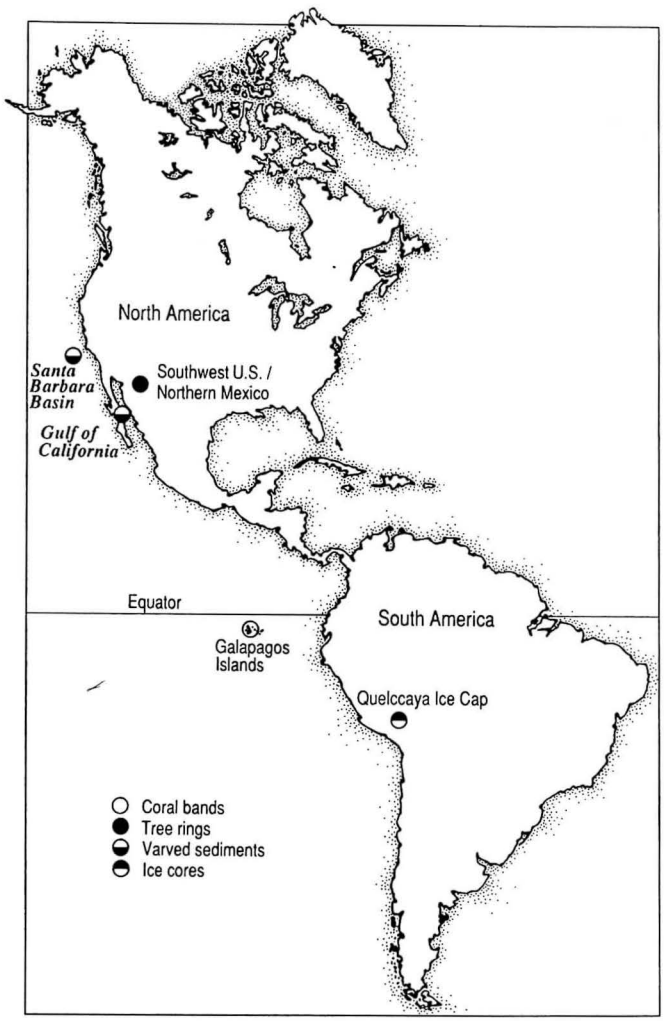

Fig. 2. Locations and identities of the five natural recording systems described in this paper.

1983], they are all subject to interannual climatic forcing, which is ultimately linked to the same complex of large-scale climatic processes. In the following section we provide a brief background for understanding how the different geographic locations, environmental settings, and the regional and local scale climatic processes govern the formation of the proxy records discussed here.

The relative sensitivities of these systems are determined by comparison of the proxy records to an index of the Southern Oscillation and an examination of the recording responses of selected proxy variables over the period since 1935. Lengths of proxy records available for this analysis range from 20 years for the Gulf of California varves to 49 years for the Quelccaya ice cap. We have also included a short section to point out the possible distortion in high-resolution paleoclimatic reconstructions that may result from inaccuracies in the proxy chronologies.

The Origins of Natural High-Resolution Records

Quelccaya Ice Cap

The Quelccaya ice cap lies in the outer tropics in the easternmost glaciated range of the Peruvian Andes. Because of its high elevation (5670 m), compared to the surrounding terrain, local disturbances in the depositional stratigraphy and radiation balance are minimized. On Quelccaya, as over most of the Peru-Bolivian Altiplano, the southern winter is the dry season while the wet season typically extends from November to April. During the wet summer season the high Altiplano, as well as the lower atmosphere, are heated by intense solar radiation before noon when cloudiness is minimal. At lower levels relatively moist air masses are advected from the east and northeast, producing intense convection and precipitation predominantly in the afternoons. Thus the major moisture source for the wet season snowfall on Quelccaya is the Amazon Basin and ultimately the Atlantic Ocean [Thompson et al., 1979]. During the dry winter season, westerly winds predominate, blowing from the high, arid altiplano of southern Peru [Thompson et al., 1984a].

The Quelccaya summit receives roughly 3 m of new snow each year, or an annual net accumulation of 1 m of water equivalent. Deposition of wind-blown microparticles varies markedly over an annual cycle producing distinct dust layers that mark the passage of the dry season. These dust layers provide annual stratigraphic markers in the ice. The association of high particulate concentrations with the dry season is a function of: (1) high radiation receipt with little accumulation of snow (with minor sublimation

or near surface melting, insoluble particles remain on the surface), (2) dominant wind direction from the west and northwest transporting material from the dry altiplano, and (3) higher wind speeds during this period [Thompson et al., 1984a].

In addition to the variability in particle concentrations in the ice, conductivities, oxygen isotope ratios, and beta radioactivity also reflect the annual cycle of climate over Quelccaya. The dry season dust layers are associated with high particle concentrations, less negative $\delta^{18}O$ values, higher beta activities, and higher conductivities [Thompson et al., 1979]. The Quelccaya ice cap chronology has been reconstructed from two cores using the combination of all parameters exhibiting a response to the annual cycle [Thompson et al., 1985]. This chronology extends 1500 years into the past.

The resulting proxy climatic record retrieved from the ice cap represents a complex integration of local and large-scale atmospheric processes sampled at the 500 mbar level, and one sensitive to the circulation patterns over both the vast Amazon Basin to the east and the dry altiplano of southern Peru to the west. Because the occurrence of El Niño results in a marked reduction of precipitation over the ice cap, a significant relationship exists between ice accumulation and the year-to-year variability associated with the ENSO phenomenon [Thompson et al., 1984b].

Galapagos Corals

Optimal growth habitats for annually banded reef-building corals are marked by 25–28 °C water temperatures, 32–36 °/₀₀ salinities, moderate turbulence (to supply nutrients and oxygen), and high light intensity to support photosynthesis by zooxanthellate symbionts [Kinsman, 1964]. The temperature and light constraints normally restrict growth of these corals to tropical latitudes at shallow ocean depths (0–50 m), although outliers may exist in temperate latitudes where warmed by western boundary currents (e.g. Bermuda).

Although seasonal changes in environmental conditions are mild in the tropics, they provide adequate stimuli for temporal growth cycles in corals expressed as a pair of low- and high-density $CaCO_3$ layers (aragonite) spanning 4–20 mm in combined thickness [Buddemeir and Kinzie, 1976]. Seasonal changes in temperature and insolation have most often been linked to banding. Typically, high-density calcification occurs during periods of warm water temperature and high cloud cover [Buddemeir et al., 1974]. Exceptions to the timing of high-density calcification with respect to insolation, however, suggest that the warm water temperature/high density relationship is the more important [Fairbanks and Dodge, 1979].

Environmental histories of the coral growth habitats may be reconstructed from the physiological indices of band widths and densities [Dodge and Brass, 1984], as well as from the variations in stable isotopes [Fairbanks and Dodge, 1979; Druffel, 1985] and minor and trace element constituents. The proxy climatic record from the Galapagos Islands, described here, was obtained from the coral reef at San Cristobal Island. Annual growth increments for these corals (*Pavona clavus*) average 11 mm with narrow high-density bands representing accretion during northern summer. Although the present reconstruction only covers a recent 33-year period, the corals have the potential to provide high-resolution chronologies extending through the past several centuries.

The proxy record consists of the variation in the trace element cadmium, which substitutes for calcium in the aragonite lattice [Shen and Boyle, 1988]. Cadmium is a nutrient analog whose concentration in the near surface waters varies with the fertility of upwelled water along the equator in the eastern Equatorial Pacific [Shen et al., 1987]. The cadmium stratigraphy reflects the reduced concentration of nutrients in upwelled waters occurring during El Niño episodes and the greater availability of nutrients during anti-El Niño periods. Nutrient deprivation during El Niño years is caused by a deepening of the nutricline associated with displacement of the thermocline below the source of upwelling [Barber and Chavez, 1983].

Tree-Rings of the Southwestern United States and Northern Mexico

Most trees in extra-tropical regions form one growth ring each year. Each ring is delimited by differences in color and density between light, thin-walled cells produced early in the growing season and dark, thick-walled cells produced late in the growing season. The thickness, wood density, and isotopic composition of an annual ring all provide climatic information when tree growth is strongly dependent upon one or two environmental conditions (normally temperature and soil moisture), which are closely linked to regional climatic variability [Fritts, 1976, Chapters 1, 2, and 9].

Trees near the edge of their distributional range are more sensitive to a single limiting factor than are those in the middle of their range. Throughout most of western North America the southern forest boundary is determined primarily by moisture stress, so growth indices from the subtropical limits of their species range reflect variability in precipitation. Reconstruction of a proxy climatic signal from tree rings also requires careful attention to sample site selection in order to minimize nonclimatic effects such as fire, disease, and proximity to the water table (i.e., well drained slopes versus valley floors). These effects are further reduced by averaging indices from several trees within and among sites as well as comparison of different species to identify growth response to the limiting climatic variable. Ring widths are also a function of the age of the tree (decreasing with age). This nonclimatic effect is removed by fitting and subtracting a growth curve [Fritts, 1976, Chapter 6] from the annual ring widths of a tree.

Dendrochronologies are reconstructed by cross-dating of multiple cores from as many trees as practical within a site [Fritts, 1976, Chapters 1 and 6]. This procedure of matching distinctive ring width patterns among cores minimizes the chronological error arising from missing or false rings produced by extreme weather during the middle of the growing season (addition of false ring) or stressful years unfavorable to growth (missing rings). The composite dendrochronology used in this paper (1935–1964) was obtained from seven conifer sites throughout New Mexico (4), Colorado (1), Baja California (1), and Chihuahua (1) [Michaelsen, this volume, Figure 1]. This chronology reaches back over a total period of 400 years.

Conifers in this semiarid region have been especially useful as proxy records of precipitation, streamflow, and other water related variables [cf. Stockton and Meko, 1975; Meko and Stockton, 1984]. Furthermore, precipitation in southwestern United States and northwestern Mexico is correlated with the ENSO variability [Douglas and Englehart, 1984]. Thus the tree growth indices from this region provide a reasonable proxy index to large-scale interannual climatic variability related to the ENSO cycle [Michaelsen and Daily, 1983; Lough and Fritts, 1985; Michaelsen, this volume].

Marine Varves of the Santa Barbara Basin and Gulf of California

A limited number of regions are known from the world's oceans where annually deposited (varved) sediments are presently accumulating [Seibold, 1958; Soutar and Crill, 1977; Soutar et al., 1981]. Marine varves are formed by deposition of two seasonal laminae which can be distinguished by the variation in their contents of biogenic versus detrital terrigenous components. The sites of accumulation are all characterized by oxygen deficient water, in contact with the sea floor, which inhibits the development of communities of benthic animals and would otherwise destroy the lamina structure by mixing and burrowing. These areas are located along the continental margins within silled basins, fjords, or on open continental slopes. The proximity to land provides for high rates of sedimentation controlled by contrasting seasonal climatic regimes, which produce the distinct alternation in the composition of particles arriving at the sea floor.

The two best known sites of present accumulation of these sediments within the eastern Pacific are the Santa Barbara Basin in the Southern California borderland [Soutar and Crill, 1977] and the continental slopes

of the Gulf of California [Calvert, 1966]. The rate of deposition in the upper uncompacted 10 cm of the Santa Barbara Basin is approximately 4 mm per year, while along the eastern margin of the central Gulf of California it is roughly 3 mm per year. Reconstruction of accurate modern varve chronologies requires the recovery of undisturbed sediment cores [Soutar, 1978] and cross-dating among several cores, combined with radioisotope chronologies [Baumgartner et al., 1989a]. Although varve deposition has occurred through the Holocene in both the Santa Barbara Basin [Pisias, 1978] and the Gulf of California [Soutar et al., 1982], two factors interfere with the reconstruction of long, continuous records of annual resolution. The most important for the Santa Barbara Basin is the occasional interruption of the varve record from increases in oxygen content of the bottom water (the most recent of these has significantly degraded the resolution between approximately 1750 and 1850). In the Gulf of California small but frequent discontinuities in the varve stratigraphy are produced by small-scale mass movement downslope associated with seismic activity. This problem has so far prevented the establishment of an accurate chronology in the Gulf of California extending back beyond the early years of the 20th century [Baumgartner, et al., 1989a].

In both the Santa Barbara Basin and the Gulf of California seasonal enrichment of biogenic material in the sediment is mediated by wind driven coastal upwelling [Soutar et al., 1981]. Off southern California alongshore northwesterly winds are most intense during spring and summer resulting in the upwelling of nutrient rich water into the euphotic zone and subsequent increase in phytoplankton and zooplankton productivity. These winds are associated with the seasonal strengthening and northward migration of the subtropical North Pacific high pressure cell. Within the Gulf of California the most intense coastal upwelling and biological productivity occur along the eastern margin during the winter and spring period of strong northwesterly winds, which are also related to the strength and position of the North Pacific high. The annual increase in biological productivity off southern California and in the Gulf of California results in the deposition of a lighter colored and less dense seasonal lamina.

The darker and more dense laminae in the Gulf of California and the Santa Barbara Basin are associated with a seasonal increase in the supply of terrigenous detritus from the adjacent continent. Off southern California the rainfall, which usually begins around late October and continues into April, provides a pulse of detritus over the continental shelf from the fluvial discharge. Much of this material is deposited on the shelf before reaching the basin. However, resuspension of this material, primarily during the more intense winter storms [Drake et al., 1972], promotes migration towards the basin margin. Comparison of varve thickness records to regional rainfall indicates that these intermediate processes of deposition and resuspension of terrigenous material over the shelf have the effect of smoothing the year-to-year variability in the rainfall [Soutar and Crill, 1977].

Until recently it was thought that the dark "summer" laminae in the Gulf of California were a response to the seasonal runoff from the mainland rivers. However, Baumgartner et al. [1989b] have shown that damming and control of all the principal rivers draining into the central Gulf has had no perceptible effect upon the deposition of the dark laminae (estimated from measured mass accumulation of terrigenous material from the varves). They argue that summer dust transport associated with convective thunderstorms over the arid Sonoran Desert is a more reasonable mechanism for a seasonal increase in the supply of terrigenous material than fluvial injection to the central Gulf of California. The effect of damming the rivers in the more tropical region bordering the southern Gulf of California has not been investigated.

The varved sediments in both the Santa Barbara Basin and the Gulf of California provide records of the response of the overlying coastal pelagic ecosystems to large-scale interannual climatic change. Baumgartner et al. [1985] have shown that the year-to-year variability in species composition and cell flux of siliceous phytoplankton (diatoms and silicoflagellates) recovered from the sediments of the central Gulf of California is correlated with the ENSO related climatic change. Weinheimer et al. [1986] show evidence that the variation in depositional flux of radiolarians (microzooplankton) observed from the Santa Barbara Basin varves also indicates a response to El Niño occurrences. To date stable isotope ratios have not been measured at an annual resolution from these sediments. However, intermediate-resolution proxy records from oxygen isotope ratios in biogenic material from the Santa Barbara Basin [Dunbar, 1983] and the Gulf of California [Juillet et al., 1983; Juillet-LeClerc and Schrader, 1987] suggest that these parameters should also provide high-resolution proxy climatic data.

Sensitivity of Natural Systems to Large-Scale Interannual Climatic Change

Each of the proxy systems described above has been shown to respond in some way to regional meteorological and (or) oceanographic forcing mediated by the ENSO phenomenon. We are interested here in comparing and contrasting the sensitivity of each natural system to interannual climatic variability associated with ENSO. We would also like to call attention to some of the differences among the individual proxy variables which act as separate recording channels within a given system.

These objectives can be accomplished by determining the fidelity and response characteristics of the respective proxy records to the large-scale interannual variability from an examination of their correspondence to an index of the Southern Oscillation. The Southern Oscillation Index (SOI), used here, is the difference in atmospheric pressure at sea level between the island of Tahiti and Darwin, Australia [Rasmusson and Wallace, 1983], computed as annual averages in order make the comparison with the proxy records. The SOI was constructed by first computing standardized monthly anomalies for each station, then subtracting Darwin from Tahiti, and finally calculating annual averages.

The annual SOI anomalies are plotted in standard units at the head of Figures 3 and 4. We use standard units here as a convenience to scale the variance by removing the mean of the series from each value and dividing by the standard deviation (standardized values are given in units of standard deviation). Negative values in the plots of the SOI (Figures 3 and 4) are shaded to indicate the occurrence of El Niño episodes or El Niño-type events. El Niño episodes are identified in these plots with letters corresponding to the subjective classification of their strengths (W = weak, M = moderate, S = strong, VS = very strong) according to Quinn et al. [1978 and 1987]. Note that not all negative SOI anomalies have been classified as El Niño years and that the subjective classification does not necessarily agree with the quantitative values in the SOI. For example, some events classified as weak or moderate show more negative annual SOI values than the strong 1957–1958 event.

Comparison of Natural Records to ENSO Variability

The proxy records are assembled below the SOI plots in Figures 3 and 4. Wherever available we have included two or more variables from the individual proxy systems for this comparison. Only the Quelccaya ice cap and the Santa Barbara varves have complete records extending over the 50-year period considered here. The patchy coverage shown by the other series indicates the state of progress achieved so far in their reconstruction through the mid-20th century. All the proxy series represent annual averages except for the Santa Barbara radiolarian record, which was sampled at 2-year intervals. Note also that some of the proxy variables are plotted here in standard units, but this does not bias, in any way, the comparisons; rather it reflects the individual preferences among coauthors in presentation of the their data.

The tree-ring width index shown in Figure 3 was reconstructed from the first principal component of the ring widths from the seven sites throughout southwestern United States and northern Mexico. This series was band-pass filtered to remove frequencies higher than 0.35 cycles per year

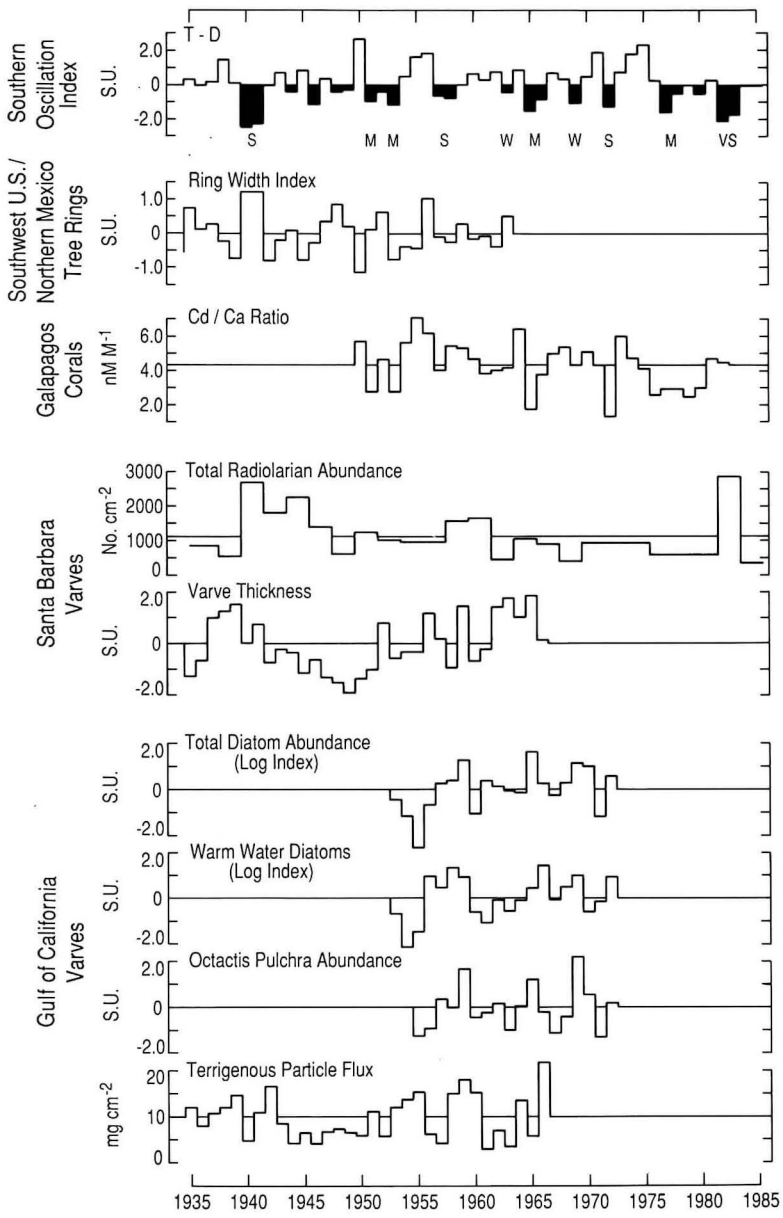

Fig. 3. Time series of proxy variables from four of the five natural systems plotted below the SOI (Tahiti minus Darwin). Negative values of the SOI are shaded and the well-defined El Niño episodes identified by letters corresponding to the subjective classification of El Niño strengths in Quinn et al. [1978 and 1987]: W (weak), M (moderate), S (strong), VS (very strong). The standard unit label on vertical axes indicates that values are plotted in units of standard deviation. Ticks on time axis correspond to month of July. See text for description of individual variables.

(cpy) and lower than 0.10 cpy. The final ring width index (plotted as standard units in Figure 3) was obtained by a multiple regression of lagged versions of the filtered series against the SOI [Michaelsen, this volume]. The Cd/Ca series in Figure 3 is the sequence of mole ratios measured from the total annual growth bands of the corals at San Cristobal Island in the Galapagos Islands [Shen et al., 1987]. The radiolarian abundance index in Figure 3 represents the calculated fluxes of all radiolarians over 2-year intervals in the Santa Barbara Basin from counts made on two successive cores (Casey, unpublished data). The varve thickness series from the Santa Barbara Basin in Figure 3 was measured from X radiographs of a sediment core, with corrections made for variations in water and salt content [Soutar and Crill, 1977] and is presented in standard units. The total diatom abundances curve, the warm water diatom index, and the *Octactis pulchra* index in Figure 3 were reconstructed from a single core from the central Gulf of California

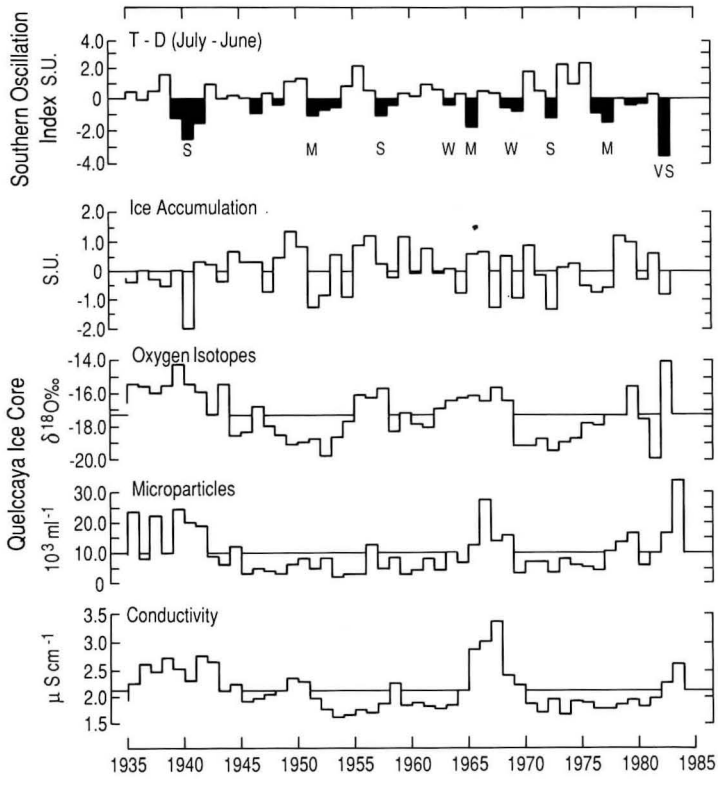

Fig. 4. Time series of proxy variables from the Quelccaya ice cap plotted below the SOI (Tahiti minus Darwin). Note that annual values for SOI calculated for July through June. Negative values of SOI shaded and El Niño episodes identified as in Figure 3. S.U. on vertical axes indicates that values are plotted in standard units. Ticks on the time axis correspond to month of July. See text for description of individual variables.

[Baumgartner et al., 1985]. The total diatom abundances and the warm water diatom species values are logarithmic transformations of the annual fluxes to the sea floor and are plotted as standard units of the log indices. The *Octactis pulchra* abundance index represents the annual flux (in standard units) of this single species (a silicoflagellate) to the sea floor. The terrigenous particle flux series in Figure 3 represents the mass accumulation of inorganic detritus in the dark laminae measured from a core in the central Gulf of California [Baumgartner et al., 1989b].

The ice accumulation curve in Figure 4 (values in standard units) is based on measurements of the annual thicknesses between dust layer separations in the two ice cores taken from Quelccaya ice cap [Thompson et al., 1985]. The oxygen isotope values, microparticle concentrations, and conductivities are averages of the sample sequences taken throughout each annual layer also averaged between the two ice cores. The microparticle values represent concentrations of the greater than 1.59 μm size fraction. Note that the SOI values in Figure 4 are averaged over the July–June interval rather than the calendar year as in Figure 3. This is done to include the wet season within one climatic year for direct comparison with the Quelccaya records.

The relative correspondence or fidelities of the different proxy systems is estimated by correlation of the individual variables in Figures 3 and 4 to the respective indices of the Southern Oscillation. Table 1 lists the coefficients for the correlations between each proxy variable and the SOI series at the centered, or zero-lag, position (central column in the table) as well as for the cross-correlations [Davis, 1973, Chapter 5) at a 1-year lag to either side of the 0 lag position. Significance levels, which are shown in parenthesis in the table, are not adjusted for autocorrelation effects in the SOI or proxy series. This means that we assume the observations within a given series to be independent from one another. Although this is not true for all of the series (see description of autocorrelation functions below), the significance levels are useful as guidelines for overall comparison of the correlations with the SOI. The lagged correlations with SOI leading (i.e., -1 lag) were calculated to determine if there is any delay in the natural recording systems. Significant correlation with SOI values trailing those of the proxy record ($+1$ lag) does not indicate that the proxy record is responding to ENSO variability, but probably indicates interference from unknown sources.

The correlations in Table 1 can be grouped into four general patterns. First, moderately high correlations at 0 lag and low correlations at the other lag positions are obtained for the tree-ring widths, Cd/Ca ratios in Galapagos corals, and the total diatom abundances, and *Octactis pulchra* values in the Gulf of California varves. These proxy indices appear to respond with minimal delay and with reasonable fidelity to the ENSO fluctuations. (Note, however, that the tree-ring index only attains this characteristic after band-pass filtering). The second group, consisting of the Santa Barbara radiolarians, and the ice accumulation, and $\delta^{18}O$ ratios from the Quelccaya ice cap, shows no indications of delay or persistence, but exhibits somewhat lower correlations at 0 lag. The third group consists of the warm water diatom index, the terrigenous flux from the Gulf of California varves, and the microparticle concentrations from the Quelccaya ice cap. These series show higher correlations at nonzero lags. The relatively high correlations

TABLE 1. Correlation Coefficients for −1, 0, and +1 Lag Correlations Between SOI and Proxy Variables from Each of the Natural Recording Systems Shown in Figures 3 and 4
[Significance levels are indicated in parenthesis after the correlation coefficients]

Record	SOI Leads: −1	0	SIO Trails: +1
Southwestern U.S. Tree-Rings			
Ring Width	0.00(NS)	−0.53(0.99)	−0.13(NS)
Galapagos Corals			
Cd/Ca Ratio	0.27(0.86)	0.58(0.99)	0.17(NS)
Santa Barbara Varves			
Total Radiolarians	0.05(NS)	−0.43(0.97)	0.10(NS)
Thickness	0.14(NS)	−0.07(NS)	−0.25(0.82)
Gulf of California Varves			
Total Diatoms	−0.02(NS)	−0.63(0.99)	−0.16(NS)
Warm Water Diatoms	0.13(NS)	−0.40(0.92)	−0.43(0.93)
Octactis pulchra	−0.06(NS)	−0.60(0.99)	0.04(NS)
Terrigenous Flux	−0.40(0.98)	0.07(NS)	0.14(NS)
Quelccaya Ice Cap			
Ice Accumulation	−0.01(NS)	0.36(0.99)	0.04(NS)
$\delta^{18}O$	0.06(NS)	−0.31(0.97)	−0.17(NS)
Microparticles	−0.39(0.99)	−0.22(0.88)	−0.19(0.80)
Conductivity	−0.25(0.92)	−0.14(NS)	−0.05(NS)

with SOI leading terrigenous flux and the microparticles may indicate some delay in the processes which produce these records. The slightly higher correlation obtained from the warm water diatoms leading the SOI, versus that at 0 lag, is not readily interpretable. Finally, the Santa Barbara varve thicknesses and Quelccaya ice cap conductivities do not show any clear correspondence to the ENSO signal.

Analysis of the Recording Responses

The correlations in Table 1 illustrate only the general nature of the response of each record to the ENSO variability. A clearer picture of the persistence structure in the records is obtained by examination of the plots of the autocorrelation functions calculated for selected proxy variables. The autocorrelation functions [Davis, 1973, Chapter 5] point out the degree of dependency among successive values in the proxy series thus indicating whether or not there is some delay in the recording mechanisms. Scatterplots of the proxy values against the SOI provide a complement to the autocorrelation functions for a more complete description of the recording responses. Ideally, response to the ENSO variability would be best characterized using cross-spectra, but most of the proxy series are too short to obtain the necessary significance. The ice core records are, however, just long enough, and some cross-spectral results of these series are presented below.

Figure 5a indicates that there is no autocorrelation in the tree-ring width index. The original series of ring widths did, however, show a considerable

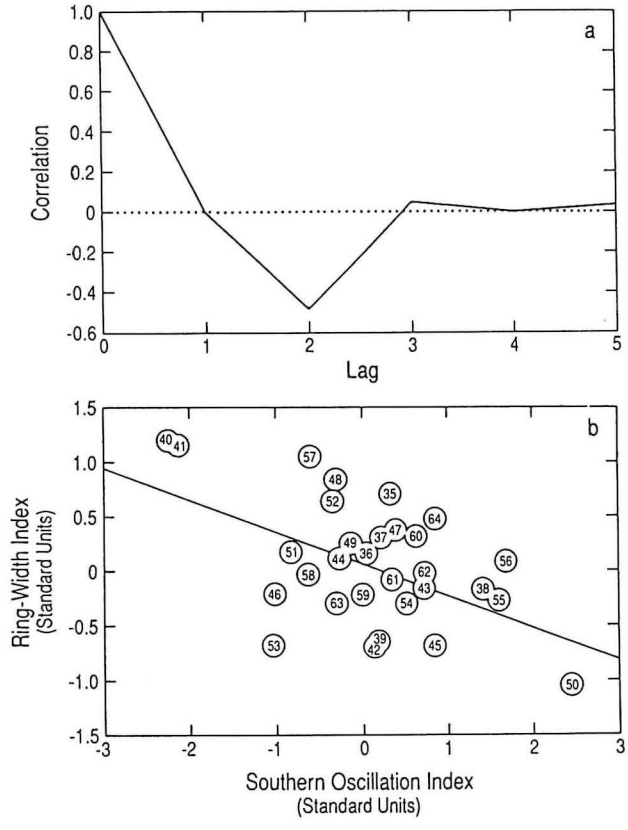

Fig. 5. (a) Autocorrelation of ring width series from tree-rings of southwestern United States and northern Mexico. (b) Scatterplot of the ring width index against SOI. Each data point on scatterplot is shown by its corresponding year to determine response of proxy variable to ENSO variability. Least squares fit shown by straight line.

degree of persistence, which was removed by the band-pass filtering mentioned above. In addition the highest correlation with the SOI occurred when the original ring width index lagged the SOI by 1 year. This effect was removed by regressing the lagged series so that there is no correlation with the SOI at nonzero lags (Table 1). Examination of the scatterplot (Figure 5b) and times-series plot (Figure 3) indicates that the ring width index is not uniformly successful at identifying El Niño years (negative values of the SOI). A strong response to the large 1940–1941 El Niño event is clearly evident in Figure 5b by the separation of these points from the remaining field of data. There is also a well defined response associated with the strongly positive SOI value for 1950, as well as for the other clear anti-El Niño years of 1938, 1955, and 1956. However, there is a less consistent response to the midrange values of the SOI (grouped between +1 and −1 standard units of the SOI) indicated by the increased scatter around the regression line in this region in Figure 5b.

The autocorrelation of the Galapagos coral record shows virtually no persistence indicating a lack of memory from one year to the next in the recording mechanism of this variable (Figure 6a). The scatterplot (Figure 6b) shows what appears to be a relatively consistent response of the Cd/Ca ratios to the ENSO variability. The relatively high Cd/Ca value for 1982, seen in Figure 6b, is probably due to sampling of the coral prior to the onset of the major warming, which began in the latter part of 1982. Note also that the 1958 value appears anomalously high for a warm year. Subsampling of the 1958 coral band yielded a significantly lower value for the first half of this year (similar to the values for 1965 and 1972) indicating that the recording response must be quite rapid. The high value for 1958 is produced by averaging over the total growth increment. The high correlation of the cadmium record to the SOI results from the lack of persistence and from a fairly uniform response of the recording mechanism over all years. Most of the El Niño and anti-El Niño years are identified with approximately equal precision.

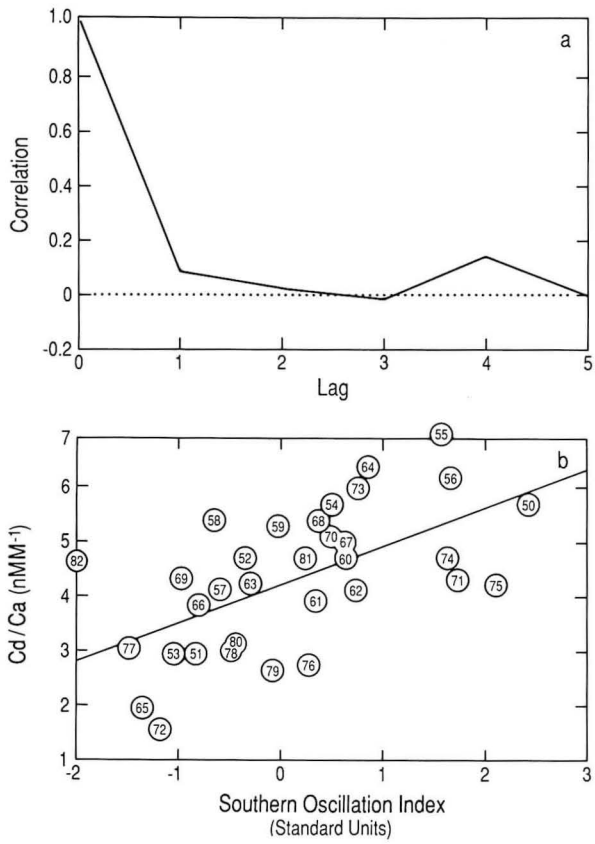

Fig. 6. (a) Autocorrelation of the Cd/Ca ratio series of Galapagos corals. (b) Scatterplot of Cd/Ca values against SOI. Data points indicated by their corresponding years. Least squares fit shown by straight line.

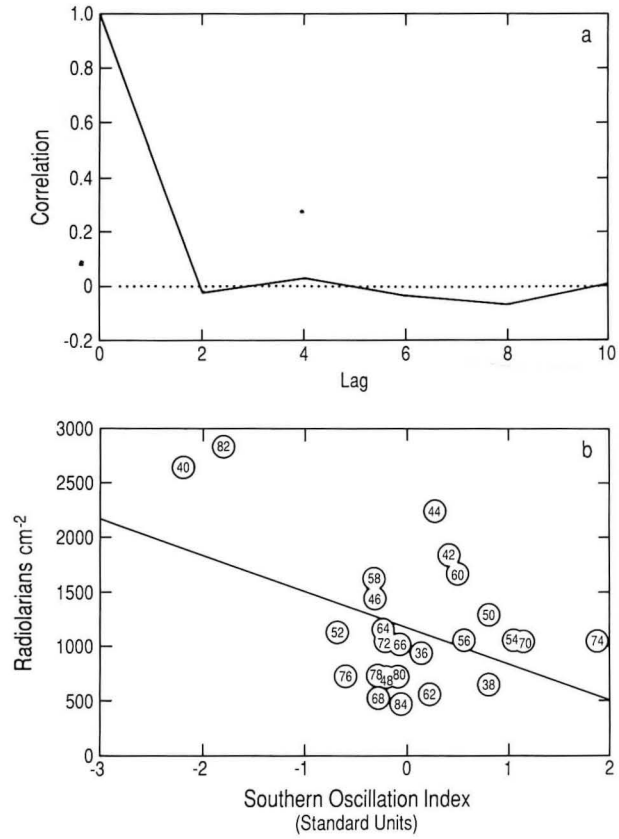

Fig. 7. (a) Autocorrelation of the radiolarian abundance index from the Santa Barbara Basin varves. The 2-year lags correspond to the 2-year sampling intervals used for this record. (b) Scatterplot of radiolarian index against the SOI. Data points indicated by the corresponding years. Least squares fit shown by straight line.

The autocorrelation of the Santa Barbara varve radiolarian record (Figure 7a), sampled at 2-year intervals, indicates that there is no persistence from one interval to the next. The fact that this record was sampled at 2-year intervals, however, has important consequences for its ability to identify individual ENSO anomalies. When the SOI is averaged over 2-year intervals (starting with even years) only the 1940–1941 and the 1982–1983 events stand out. The scatterplot (Figure 7b) shows that these two events are well resolved, but the 2-year averaging has strongly attenuated the signal in other years. This illustrates very well the importance of high-resolution sampling for identifying a response to short-period climatic variability.

The Santa Barbara varve thicknesses do have a significant level of persistence, as is evident in both the autocorrelation and time-series plots (Figure 8a and Figure 3). Soutar and Crill [1977] have shown that the varve deposition process depends upon regional rainfall over several previous years

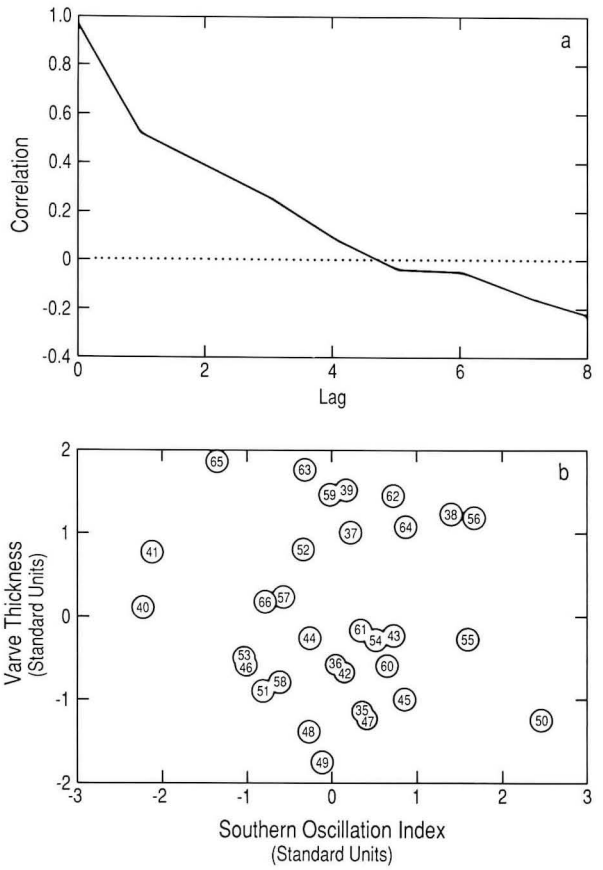

Fig. 8. (a) Autocorrelation of the varve thickness series from the Santa Barbara Basin. (b) Scatterplot of varve thicknesses against the SOI. Data points indicated by corresponding years.

(a filtering effect on the terrigenous signal associated with intermediate storage and resuspension of material over the shelf, mentioned above). As a result, the varve thickness record is a strongly smoothed version of the rainfall record. Both the scatterplot (Figure 8b) and the time-series plot (Figure 3) indicate that this record is not sensitive to the ENSO phenomenon. Undoubtedly, this is because Santa Barbara regional rainfall itself is not strongly correlated with the ENSO rather than due to the high persistence in the varve thickness record. This is a good example, therefore, of a natural system with one recording channel (total radiolarians) which is sensitive to the ENSO variability and another channel (varve thickness) which is not.

The index of total diatom abundance (cell flux) in the Gulf of California varves shows a small degree of autocorrelation (Figure 9a) with about 5 percent of the variance carrying over from the previous year. This is a somewhat higher level of persistence than is characteristic of the annual SOI, but the smoothing effect is not strong enough to produce any significant correlation at nonzero lags. Rather, the scatterplot (Figure 9b) indicates that the response of this mechanism to ENSO variability is rapid and relatively uniform over the length of the record. Both El Niño and anti-El Niño years are identified here with reasonable precision.

The record of terrigenous flux in the Gulf of California varves shows no evidence of persistence in the autocorrelation function (Figure 10a) and no overall pattern of persistence in the time-series plot (Figure 3). Thus the relatively high correlation with SOI leading terrigenous flux by 1 year (Table 1) is not produced by any smoothing effect. The scatterplot of terrigenous flux against the SOI lagged by 1 year (Figure 10b) indicates that the lag response is fairly consistent. The terrigenous flux record is apparently controlled by eolian transport [Baumgartner et al., 1989b], but there is insufficient information to relate aeolian processes in this region to ENSO variability; thus the cause of this lag relationship is still unclear.

The autocorrelation of the Quelccaya ice accumulation series (Figure 11a) shows that there is no persistence in this recording mechanism. The length of the ice core records permits us to also calculate cross-spectra with the SOI (Figure 11b). The spectra were obtained by transforming cross-covariances using a Bartlett lag window with a length of 12 years [Jenkins and Watts, 1968]. The resulting estimates have about 12 degrees of freedom. Coherence with the SOI (Figure 11b) indicates that there is a good correspondence within the main ENSO frequency band (4- to 6-year period, equivalent to 0.25 to 0.17 cpy). The correlation with SOI (0.36) is improved somewhat (0.42) by band-pass filtering the ice accumulation record, suggesting that the accumulation record contains interference from processes acting at other time scales and probably unrelated to ENSO. The scatterplot of the filtered ice accumulation record against the SOI (Figure 11c) shows that the two large events of 1982–1983 and 1940–1941 clearly stand out from the rest of the data field. Notwithstanding the considerable scatter over the remaining years, the principal El Niño occurrences are recorded with fair precision; thus the ice accumulation mechanism provides a sensi-

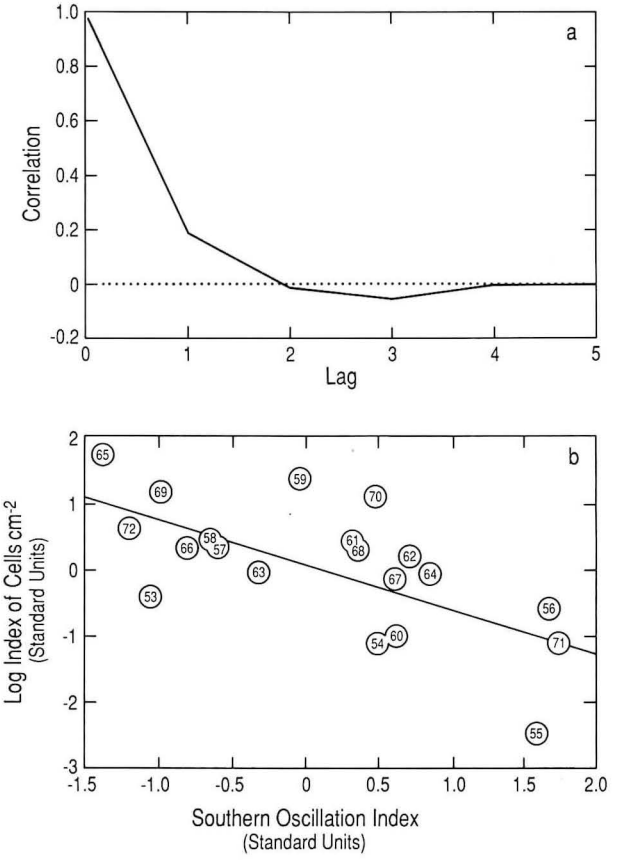

Fig. 9. (a) Autocorrelation of the diatom abundance index from the Gulf of California varves. (b) Scatterplot of the diatom abundance index against the SOI. Data points indicated by corresponding years. Least squares fit shown by straight line.

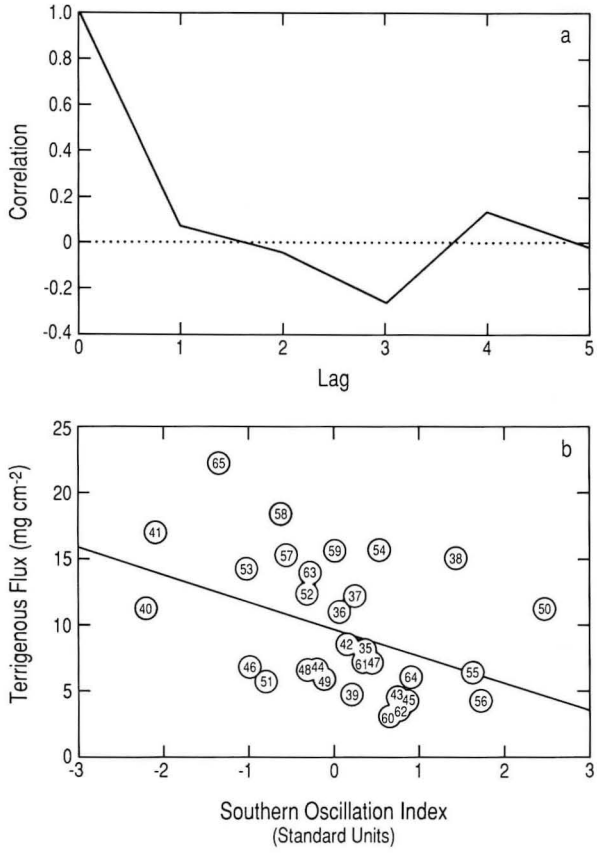

Fig. 10. (a) Autocorrelation of the terrigenous flux series from the Gulf of California varves. (b) Scatterplot of the terrigenous flux index against the SOI. Least squares fit shown by straight line.

tive record of large events and shows a somewhat weakened, but still useful, sensitivity to the overall ENSO variability.

The oxygen isotope ratios from the Quelccaya ice cap show considerable persistence with positive autocorrelations out to 4 lags (Figure 12a). As a result, the autospectrum of the $\delta^{18}O$ record (Figure 12b) shows most of the variance concentrated in frequencies less than 0.10 cpy (periods longer than 10 years). The autospectrum of the SOI (also plotted on Figure 12b), on the other hand, has very little variance at low frequencies and shows the characteristic ENSO peak at the 4 to 6 year time scale. The $\delta^{18}O$ spectrum has a trough in the main ENSO frequency band and insignificant coherence (not shown here) with the SOI in this band. The moderate correlation between the two records (Table 1) is apparently produced by some coherence in frequencies higher than the main ENSO signal (periods shorter than 3 years). Thus the $\delta^{18}O$ recording mechanism does not seem to be very sensitive to ENSO activity.

The record of microparticle concentrations in the ice also shows a high degree of persistence with positive autocorrelations to 5 lags (Figure 13a). This persistence is also evident in the cross-correlations with the SOI which are negative for all 3 lags shown in Table 1. Significant coherence between the two series (Figure 13b) is limited to frequencies lower than 0.10 cpy (periods greater than 10 years). This might indicate that the microparticle record is responsive to some component of SOI variability which is not associated with the dominant ENSO frequency. If this is true, the microparticle record may be useful for characterizing longer term behavior of the Southern Oscillation.

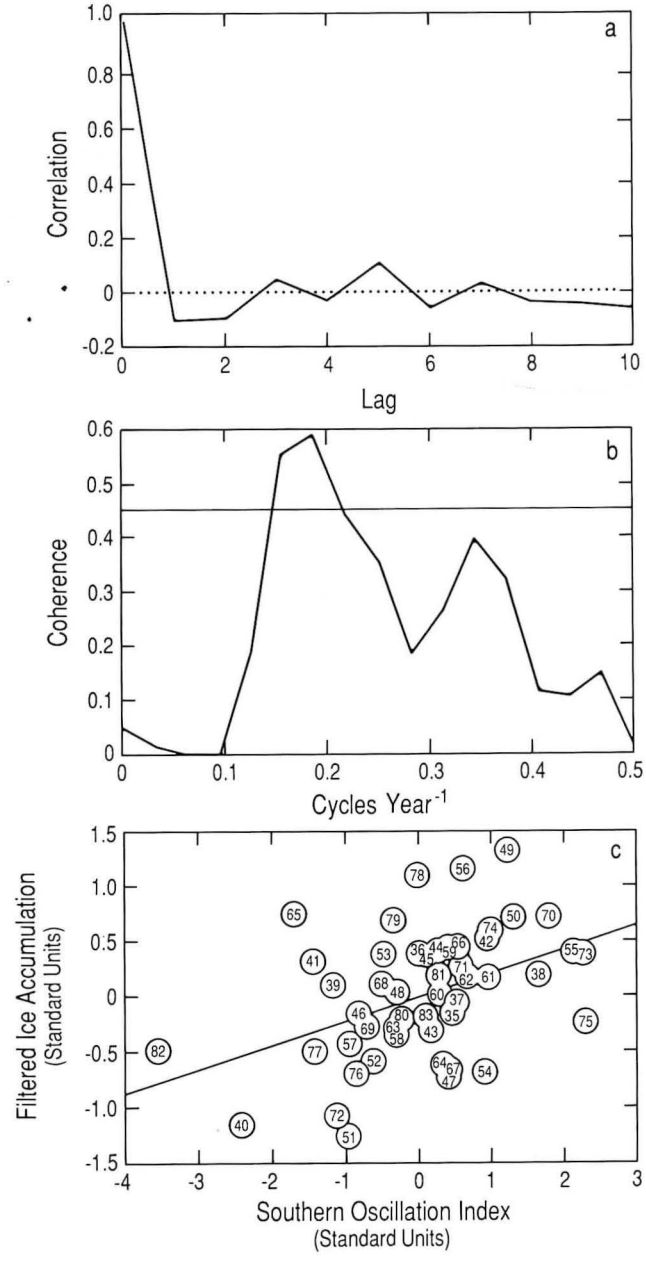

Fig. 11. (a) Autocorrelation of the ice accumulation record from the Quelccaya ice cap. (b) Cross-spectral coherence between the ice accumulation series and the SOI. The 95 percent significance level is indicated by horizontal line. (c) Scatterplot of the ice accumulation series and the SOI. Note that ice accumulation series has been band-pass filtered resulting in slightly improved relationship (see text). Least squares fit shown by straight line.

Effects of Chronological Error on Paleoclimatic Reconstructions

There are two fundamental assumptions implicit in the foregoing analyses of the proxy records. These are (1) the stratigraphic markers produced by the recording systems accurately reflect the annual climatic cycle and (2) our techniques of observation are adequate to identify the proper time marks

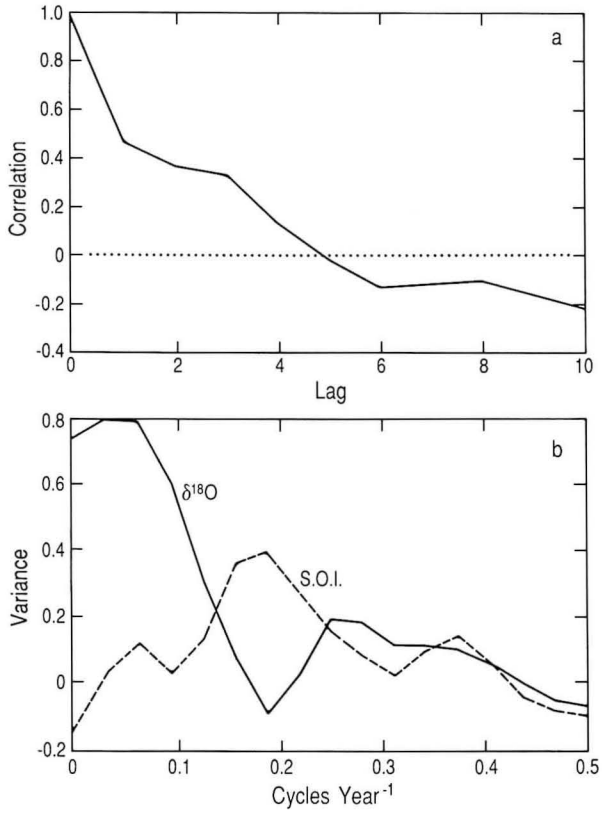

Fig. 12. (a) Autocorrelation of the $\delta^{18}O$ record from the Quelccaya ice cap. (b) Autospectrum of the $\delta^{18}O$ series plotted with that of the SOI.

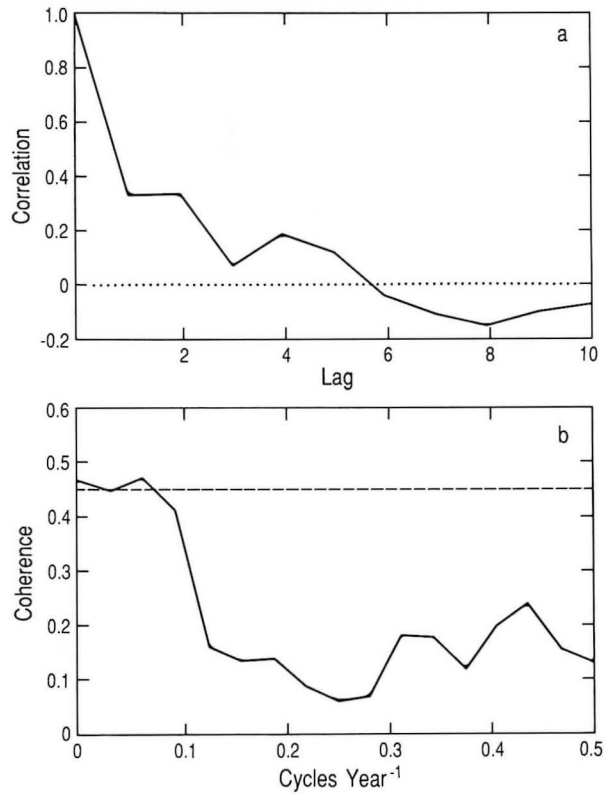

Fig. 13. (a) Autocorrelation of the microparticle record from the Quelccaya ice cap. (b) Cross-spectral coherence between the microparticle series and the SOI. Horizontal line indicates 95 percent level of significance.

(and reject any spurious ones). These assumptions permit us to fix a date to each of the proxy values measured from a recording system. It is, therefore, important to understand the repercussions stemming from an inaccurate chronology that violates these assumptions. We can achieve this by illustrating the potential distortion of the paleoclimatic signal associated with chronological errors that might be introduced into the records by a combination of inaccurate sampling and natural perturbations. With the exception of the efforts in dendrochronology [e.g., Holmes et al., 1986] there does not seem to have been a great deal of attention focused on the effects of imperfect chronologies that result from overlooking the occurrence of missing or false annual values in the natural records. However, any attempt at the reconstruction of accurate high-resolution chronologies should take these effects into account [Wendland, 1975; Baumgartner and Christensen, 1978].

To demonstrate these effects we have generated a synthetic proxy record to mimic a natural paleoclimatic reconstruction of ENSO variability (Figure 14). This was done by adding a random component to a 116-year "parent" SOI used in Michaelsen [this volume]. The synthetic record shares 50 percent of the variance with the true SOI (correlation of 0.70), so it is comparable to a very high quality natural proxy record. The synthetic proxy record was then perturbed by removing values or adding extra values at randomly selected positions. This mimics the real problem of missing or false years occurring in the proxy records. To examine the effect of these perturbations we compare cross-correlations of the perturbed proxy records with the parent SOI to the original cross-correlation of the unperturbed synthetic record with the parent SOI. Each experiment was repeated 100 times for 1, 2, and 3 missing and false years in order to generate a distribution of correlations. In all cases the upper ends (youngest values)

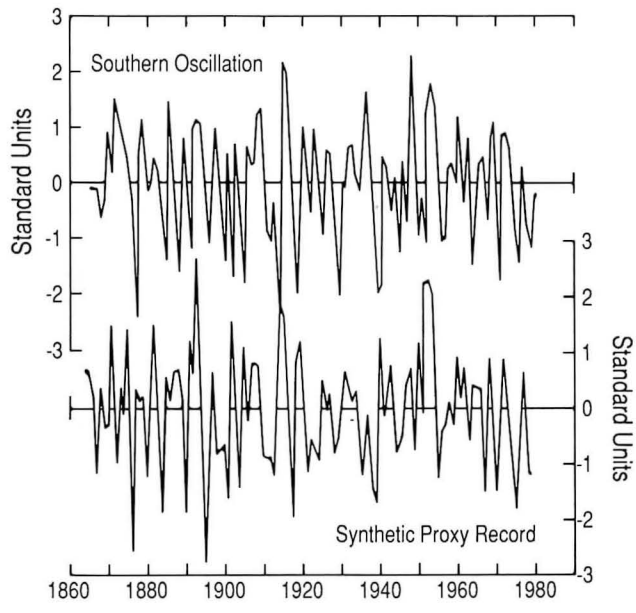

Fig. 14. Comparison of SOI (upper curve) to a synthetic proxy record obtained by adding a random component to the SOI. Correlation between the synthetic proxy record and its parent SOI is 0.7. Curves represent 116 annual values.

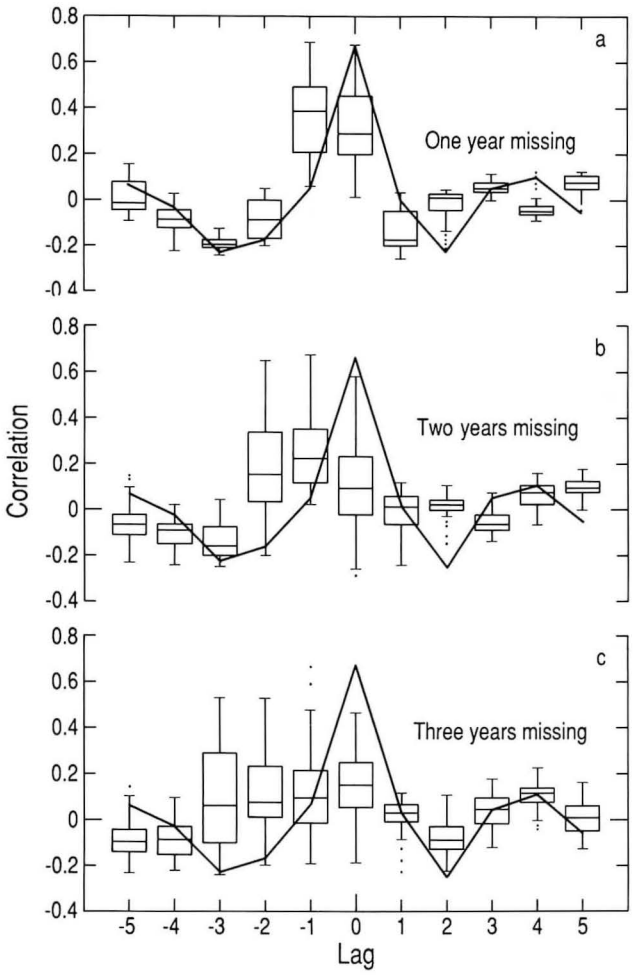

Fig. 15. Results of experiments to model the effects on the cross-correlation with parent SOI produced by missing years in the chronology of the synthetic proxy record. Heavy solid line shows cross-correlation function between SOI and the unaltered proxy record. The boxplots indicate the distributions of correlations (see text) for each lag produced by 100 repititions of altering the proxy record (shortening) by random omission of 1, 2, and 3 years.

of the perturbed series were held fixed in the correct position relative to the SOI. This procedure also mimics the normal situation in which errors accumulate down the record.

Figure 15 shows the results of removing years, while Figure 16 shows the effect of adding false years. The solid lines in the figures represent the cross-correlation function of the unperturbed series with the SOI. The boxplots at each lag show the range and distribution of correlations obtained from the 100 repetitions of each experiment [after Tukey, 1977]. The horizontal line within each box is the median correlation; the outer edges of each box are the upper and lower quartiles, meaning that the central 50 percent of the distribution is contained within the boxes. The total range of the correlations is given by the endpoints of the vertical lines extending from the boxes except for extreme values, which are plotted separately.

The effect of removing 1 year from the proxy series (Figure 15a) is to immediately reduce the 0-lag correlation considerably and increase the negative lag 1 correlation (SOI leading) by a comparable amount. Note that the degree of distortion depends on the position of the omitted value. Errors at the lower (older) end of the record produce a negligible effect, while errors at the upper (younger) end have the strongest effect (i.e., the chronological error is propagated downward from younger to older sections of record). This produces a potentially spurious lag relationship which might be misinterpreted as a real characteristic of the recording system. For example, this might explain the lag relationship between the Gulf of California terrigenous flux record and the SOI.

When 2 years are omitted (Figure 15b) the original 0-lag correlation is smeared from lag 0 to negative lag 2 and seriously degrades the correspondence between the two series. The omission of three values (Figure 15c) further degrades the relationship as the correlation is smeared between lag 0 and negative lag 3. At this point the correspondence would be extremely difficult to identify.

The effect of inserting one, two, and three extra values (Figure 16a, b, and c) is essentially the same as omitting years except that an apparent correspondence is created with the synthetic proxy record leading the parent SOI. In one sense this is a less dangerous situation because a proxy record

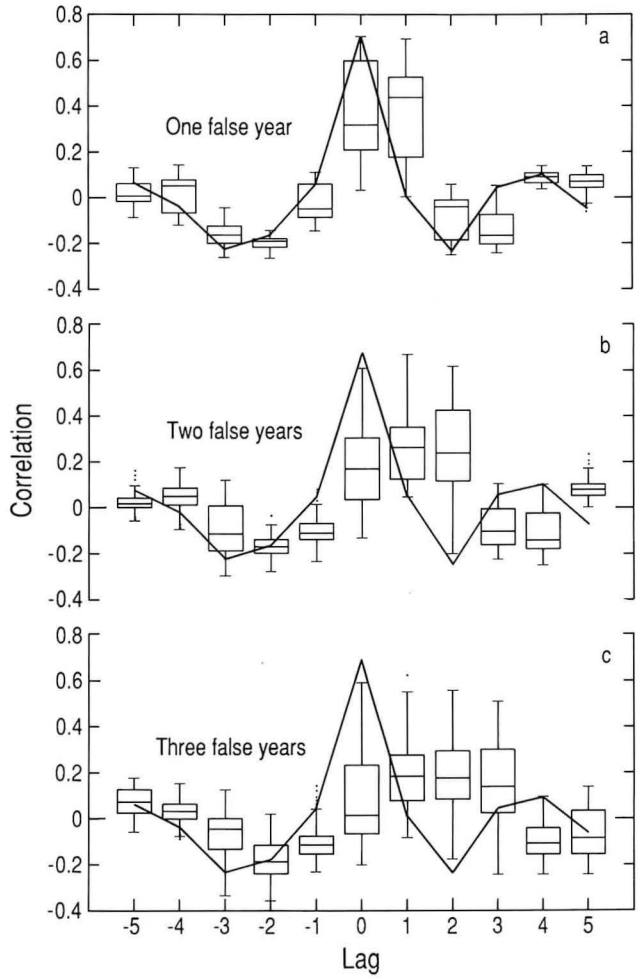

Fig. 16. Results of experiments to model effects on the cross-correlation with the parent SOI produced by false years in the chronology of the synthetic proxy record. Heavy line (equivalent to that in Figure 15) indicates cross-correlation function for the SOI and the unaltered proxy record. Box plots show distributions of the resulting correlations at each lag as in Figure 15. Experiments consisted of performing 100 repititions of randomly adding one, two, and three false values.

which lags the SOI might be accepted as genuine, while one which leads the SOI would immediately be considered suspect.

The results of this short experiment indicate that a chronological error as small as a single year (less than 1 percent of this record) can seriously complicate the interpretation of the response of the proxy recording system to climatic forcing. Furthermore, a chronological error of less than 3 percent of the total record can completely degrade what is otherwise an accurate proxy record of climatic variability.

Discussion and Conclusions

The pervasive influence of the ENSO on ocean and atmospheric circulation leaves a strong imprint on the high-resolution proxy records from the eastern Pacific and western Americas. These records are produced by a wide range of natural systems, including the tropical Quelccaya ice cap, Galapagos corals, semiarid forests of the southwestern United States and northern Mexico, and varved sediments of the Gulf of California and the Santa Barbara Basin. Analysis of the sensitivity and response of individual proxy records to the ENSO variability provides a basis for comparison among the five recording systems and among individual variables for some of the systems.

Systems exhibiting the highest fidelity are those with low persistence which have a rapid response in the frequency band of the ENSO variability. The most highly sensitive proxy records have been shown to be the Cd/Ca ratios in the Galapagos corals, the processed ring widths of the southwestern United States and northern Mexico tree-ring series, and the total diatom abundances in the Gulf of California varves. These variables are sensitive to ENSO anomalies in most years and should yield reasonable confidence in year-by-year reconstructions. The filtered Quelccaya ice accumulation record is somewhat less sensitive, but still shows a consistent response to much of the ENSO variability. This slight decrease in sensitivity is more than compensated for by the fact that the Quelccaya ice cap record is by far the longest high-resolution proxy record of ENSO behavior currently available, extending back roughly 1500 years.

The Santa Barbara radiolarian record appears to be sensitive to some of the larger events, but otherwise does not show a uniform response to the full range of ENSO variability. In its present form it might be useful for identifying the occurrence of major events affecting the California Current. The ability of this record to resolve ENSO variability is undoubtedly hampered by the 2-year sampling interval, and it is possible that 1-year sampling might provide a more accurate representation over a wider range of ENSO variability.

The natural record of climatic change may also be enhanced by several kinds of treatment of the proxy variables. These include spatial averaging of a single variable from different sites and filtering of the time series to focus on the variance within a specific frequency band. Processing of the original tree-ring width values has been the most extensive for any of the data presented here and was designed to reduce the interference in the natural system unrelated to ENSO variability. It is, therefore, interesting to note that the Cd record in the corals and the diatom index of the Gulf of California varves show a similar level of sensitivity to ENSO variability without this treatment. Sensitivity of the mass accumulation from the Quelccaya ice cores was slightly improved by band-pass filtering. On the other hand the correspondence of the Santa Barbara Basin varve thicknesses to the SOI was not improved by filtering.

The natural proxy variables which are most sensitive to the large-scale climatic change appear to be those whose response is limited primarily to a single environmental process, which is itself strongly coupled to the large-scale climate. Workers in dendrochronology have long stressed the importance of developing tree-ring chronologies which provide maximum sensitivity to a single climatic variable [Fritts, 1976, Chapters 1 and 5]. The tree-ring sites used in this study were specifically chosen for their sensitivity to moisture availability. The climatic sensitivity of the cadmium record in the Galapagos corals suggests that it must also represent a fairly straightforward response to ocean fertility.

The climatic sensitivity of the phytoplankton record preserved in the Gulf of California may indicate a similar control by a single factor, even though there is a large array of environmental variables affecting phytoplankton growth (e.g., ocean temperature, salinity, light, nutrient supply, which is itself largely dependent upon wind driven stirring, and sources of the water masses). Over annual and interannual time scales variability in the phytoplankton production is strongly dependent upon nutrient flux to the euphotic zone. The supply of nutrients in the central Gulf, in turn, appears to be closely linked to the occurrence of El Niño, although in an opposite sense as that observed along the equator [Baumgartner, 1987]. Thus interannual change in ocean fertility may also be the primary environmental forcing for the phytoplankton record in the Gulf of California varves.

Finally, it must be remembered that no matter how great the sensitivity of a natural system to interannual climatic change may be, the validity of the paleoclimatic record still depends upon the care exercised to develop a proper time series of the proxy values. The analysis of the effects of chronological error has been included here to provide a quantitative demonstration of the distortion of the climatic signal by progressively debasing the accuracy of the time signal. This provides a warning against overlooking the primary importance of reconstruction of accurate chronologies as the basis for developing paleoclimatic histories from proxy data.

Acknowledgments. We would like to thank David Peterson and James Gardner for their encouragement and support for our undertaking of this work. We are also grateful to the U.S. Geological Survey, which provided travel funds making direct communication possible among the coauthors. Critical reviews by Steve Calvert, Walter Dean, and one anonymous reviewer have lead to substantial improvement in the final manuscript. We also wish to thank Carmen de Jesús for help with typing and José Ma. Domíngues for drafting.

References

Barber, R. T. and Chavez, F. P., Biological consequences of El Niño, *Science*, v. 222, p. 1203–1210, 1983.

Baumgartner, T. R., High resolution paleoclimatology from the varved sediments of the Gulf of California, Ph.D. thesis, 287 p., Oregon State University, Corvallis, OR, 1987.

Baumgartner, T. R., and Christensen, N., An improved cross-correlation technique for cross-dating varve series taken from different sediment coring sites within a small study area, *Ciencias Marinas*, v. 5, p. 119–136, 1978.

Baumgartner, T. R., Ferreira-Bartrina, V., Cowen, J., and Soutar, A., Reconstruction of a 20th-century varve chronology from the central Gulf of California, in *The Gulf and Peninsular Province of the Californias*, edited by J. P. Dauphin and B. Simoneit, American Association of Petroleum Geoleologist, Memoir, Tulsa, OK, in press, 1989a.

Baumgartner, T. R., Ferreira-Bartrina, V., and Moreno-Hentz, P., Varve formation in the central Gulf of California: A reconsideration of the origin of the dark laminae from the 20th-century varve record, in *The Gulf and Peninsular Province of the Californias*, edited by J. P Dauphin and B. Simoneit, American Association of Petroleum Geologists Memoir, Tulsa, OK, in press, 1989b

Baumgartner, T. R., Ferreira-Bartrina, V., Schrader, H., and Soutar, A. A 20-year varve record of siliceous phytoplankton variability in the central Gulf of California, *Marine Geology*, v. 64, p. 113–129, 1985.

Buddemeier, R. W., and Kinzie, R. A., Coral growth, *Oceanography Marine Biology Annual Review*, v. 14, p. 183–225, 1976.

Buddemeier, R. W., Margos, J. E., and Knutson, D. W., Radiographic studies of reef coral exoskeletons: Rates and patterns of coral growth,

Journal of Experimental Marine Biology Ecology, v. 14, p. 177–200, 1974.

Calvert, S. E., Origin of diatom-rich, varved sediments from the Gulf of California, *Journal of Geology*, v. 76, p. 546–565, 1966.

Cane, M., Oceanographic events during El Niño, *Science*, v. 222, p. 1189–1195. 1983.

Davis, J. C., *Statistics and Data Analysis in Geology*, J. Wiley and Sons, Inc., New York, NY, 550 p., 1973.

Dodge, R. E., and Brass, G. W., Skeletal extension, density, and calcification of the reef coral, *Montastrea annularis*: St. Croix, U.S. Virgin Islands, *Bulletin of Marine Science*, v. 34, p. 288–307, 1984.

Douglas, A. V., and Englehart, P., Factors leading to the heavy precipitation regimes of 1982 83 in the United States, *Proceedings Eighth Annual Climate Diagnostics Workshop*, p. 42–54, 1984.

Drake, D. E., Kolpack, R. L., and Fischer, P. J., Sediment transport on the Santa Barbara-Oxnard Shelf, Santa Barbara Channel, California, in *Shelf Sediment Transport: Process and Pattern*, edited by D. J. P. Swift et al., Dowden, Hutchinson, and Ross, p. 307–331, Stroudsburg, PA, 1972.

Druffel, E. M., Detection of El Niño and decade time scale variations of sea-surface temperature from banded coral records: Implications for the carbon dioxide cycle, in *The Carbon Cycle and Atmospheric CO_2: Natural Variations Archean to Present*, edited by E. T., Sundquist and W. S. Broecker, p. 111–122, American Geophyical Union, Washington, DC, 1985.

Dunbar, R. B., Stable isotope record of upwelling and climate from Santa Barbara Basin, California, in *Coastal Upwelling: Its Sediment Record, Part B.*, edited by J. Thiede and E. Suess, p. 217–246, Plenum Press, New York, NY, 1983.

Fairbanks, R. G., and Dodge, R. E., Annual periodicity of the $^{16}O/^{18}O$ and $^{12}C/^{14}C$ ratios in the coral *Montastrea annularis*, *Geochimica et Cosmochimica Acta*, v. 43, p. 1009–1020, 1979.

Fritts, H. C., *Tree Rings and Climate*, 567 p., Academic Press, London, 1976.

Holmes, R. L., Adams, R. K., and Fritts, H. C., *Tree-Ring Chronologies of Western North America: California, Eastern Oregon and Northern Great Basin, Chronology Series VI*, 182 p., University of Arizona, Tucson, AZ, 1986.

Jenkins, G. M., and Watts, D.G., *Spectral Analysis*, Holden-Day, Oakland, CA, 525 p., 1968.

Juillet, A., Labeyrie, L. D., and Schrader, H., Oxygen isotope composition of diatom and silicoflagellate assemblage changes in the Gulf of California: A 700-year upwelling study, in *Coastal Upwelling: Its Sedimentary Record, Part B*, edited by J. Thiede and E. Suess, Plenum Press, New York, NY, p. 277–294, 1983.

Juillet-LeClerc, A. and Schrader, H., Variations of upwelling intensity recorded in varved sediment from the Gulf of California during the past 3000 years, *Nature*, v. 329, p. 146–149, 1987.

Kinsman, D. J. J., Reef coral tolerance of high temperatures and salinities, *Nature*, v. 202, p. 1280–1283, 1964.

Lough, J. M., and Fritts, H. C., The Southern Oscillation and tree rings: 1600–1961, *Journal of Climate and Applied Meteorology*, v. 24, p. 952–956, 1985.

Meko, D. M. and Stockton, C. W., Secular variations in streamflow in the western United States, *Journal of Climate and Applied Meteorology*, v. 23, p. 889–897, 1984.

Michaelsen, J., Long-period fluctuations in El Niño amplitude and frequency reconstructed from tree-rings, this volume, 1989.

Michaelsen, J., and Daily, J. T., Long-period modulation of El Niño, *Proceedings Eighth Annual Climate Diagnostics Workshop*, p. 140– 147, 1983.

Pisias, N. G., Paleoceanography of the Santa Barbara Basin during the last 8000 years, *Quaternary Research*, v. 10, p. 366–384, 1978.

Quinn, W. H., Neal V.T., and Antunez de Mayolo, S.E., El Niño occurrences over the past four and a half centuries, *Journal of Geophysical Research*, v. 92, no. C13, p. 14449–14462, 1987.

Quinn, W. H., Zopf, D. O., Short K. S., and Kuo Yang, R. T. W., Historical trends and statistics of the Southern Oscillation, El Niño, and Indonesian droughts, *Fishery Bulletin*, v. 76, no. 3, p. 663–678, 1978.

Rasmusson, E. M., and Wallace, J.M., Meteorological aspects of the El Niño/Southern Oscillation, *Science*, v. 222, p. 1195–1202, 1983.

Seibold, E., Jahreslagen in sedimenten der mittleren Adria, *Geologischen Rundschau*, v. 47, p. 100–117, 1958.

Shen, G. T., and Boyle, E. A., Determination of lead, cadmium, and other trace metals in annually-banded corals, *Chemical Geology*, v. 67, p. 47–62, 1988.

Shen, G. T., Boyle E. A., and Lea, D. W., Cadmium in corals: Chronicles of historical upwelling and industrial fallout, *Nature*, v. 328, p. 794–796, 1987.

Soutar, A., Collection of benthic sediment samples, southern California baseline study, Benthic Year II. *Final Report, U.S. Bureau of Land Management*, v. 2, pt. 4, 54 p., 1978.

Soutar, A., and Crill, P. A., Sedimentation and climatic patterns in the Santa Barbara Basin during the 19th and 20th centuries, *Geological Society of America Bulletin*, v. 88, p. 1161–1172, 1977.

Soutar, A., Johnson, S. R., and Baumgartner, T. R., In search of modern depositional analogs to the Monterey Formation, in *The Monterey Formation and Related Siliceous Rocks of California*, edited by R. E. Garrison and K. Pisciotto, Special Publication, Society of Economic Paleontologists and Mineralogists, Pacific Section, p. 123–147, 1981.

Soutar, A., Johnson, S. R., Taylor, E. and Baumgartner, T. R., X-radiography of Hole 480: Procedures and results, in, *Initial Reports*, DSDP, v. 64, pt. 2, edited by J. R. Curray and D. Moore, p. 1183–1190, 1982.

Stockton, C. W. and Meko, D.M., A long-term history of drought occurrence in western United States as inferred from tree-rings, *Weatherwise*, v. 28, p. 244–249, 1975.

Thompson, L. G., Hastenrath, S., and Morales Arnao, B., Climatic ice core records from the tropical Quelccaya ice cap, *Science*, v. 203, p. 1240–1243, 1979.

Thompson, L. G., Mosley-Thompson, E., Bolzan, J. F., and Koci, B. R., A 1500-year record of tropical precipitation in ice cores from the Quelccaya ice cap, Peru, *Science*, v. 229, p. 971–973, 1985.

Thompson, L. G., Mosley-Thompson, E., Grootes, P. M., Pourchet, M., and Hastenrath, S., Tropical glaciers: Potential for ice core paleoclimatic reconstructions, *Journal of Geophysical Research*, v. 89, p. 4638–4646, 1984a.

Thompson, L. G., Mosley-Thompson E., and Morales Arnao, B., El Niño-Southern Oscillation events recorded in the stratigraphy of the tropical Quelccaya ice cap, Peru, *Science*, v. 226, p. 50–53, 1984b.

Tukey, J. W., *Exploratory Data Analysis*, Addison-Wesley, Reading, MA, 499 p., 1977.

U.S. Committee for Global Atmospheric Research Program, *Understanding Climatic Change: A Program for Action, Appendix A.*, National Academy of Sciences, Washington, DC., p. 127–195, 1975.

Weinheimer, A. L., Carson, T. L., Wigley C. R., and Casey, R. E., Radiolarian responses to Recent and Neogene California El Niño and anti-El Niño events. *Palaeogeography, Palaeoclimatology, Palaeoecology*, v. 53, p. 3–25, 1986.

Wendland, W. M., An objective method to identify missing or false rings, *Tree-Ring Bulletin*, v. 35, p. 41–47, 1975.